SB³C2020
Summer Biomechanics, Bioengineering and Biotransport Conference
June 17-20, Vail, CO, USA

EFFECT OF FIBER-MATRIX INTERFACIAL STIFFNESS GRADIENT ON ANNULUS FIBROSUS FAIULURE MECHANICS

Minhao Zhou (1), Eric Neubauer Vickers (2), Grace D. O'Connell (1,3)

(1) Department of Mechanical Engineering
University of California, Berkeley
Berkeley, CA, United States

(2) Department of Molecular & Cell Biology
University of California, Berkeley
Berkeley, CA, United States

(3) Department of Orthopaedic Surgery
University of California, San Francisco
San Francisco, CA, United States

INTRODUCTION

Mechanical gradients at the hard-soft interface in fiber-reinforced biological tissues manipulate local stress-strain distributions, creating systems that can withstand large loads and deformations. At the tendon-bone interface, the elastic modulus (modulus) gradient shows a minimum compared to the modulus of tendon and bone [1]. In human intervertebral discs, the radial mechanical gradient resulted from the radial biochemical composition gradient presumably improves the disc's load-bearing capability [2-4]. Recently, bioinspired mechanical gradient designs are widely incorporated in novel engineering systems for improved mechanical performance, such as a multicore-shell structure that are stiff and tough, and a 3D printed heterogeneous system with tunable failure properties [3, 5]. However, the understanding of the interplay of local mechanical gradient and bulk mechanics has been lacking due to variations in tissue architecture and loading conditions. Furthermore, due to challenges in conducting sub-tissue level tests, the fiber-matrix interfacial mechanical gradient has not been investigated.

Finite element models (FEM) can predict three-dimensional stress-strain distributions in complex, fiber-reinforced tissues. We recently developed and validated a novel multiscale, structure-based model, which can be adapted to incorporate a mechanical gradient at the fiber-matrix interface [6]. We hypothesized that similar to the observed tissue level interfacial mechanical gradient, there existed a sub-tissue level mechanical gradient at the fiber-matrix interface that delayed tissue damage initiation while prevented tissue damage propagation. Therefore, the objective of this study was to study the effect of sub-tissue level interfacial mechanical gradient on tissue failure mechanics.

METHODS

Finite element models were developed representing three-lamellae rectangular circumferential-axial AF specimens (dimensions: 4.0, 1.0, 0.6 mm in length, width, thickness). A fiber-matrix mechanical gradient was incorporated by including a 0.01 mm-thick interfacial layer (IL, Fig. 1A–gray region). The matrix (Fig. 1A–diagonal region) was further divided into two regions: a 0.01 mm-thick inner matrix layer (IML, Fig. 1A–a) and matrix (Fig. 1A–b); fibers (Fig. 1A–dotted region) were similarly divided into a 0.01 mm-thick outer fiber layer (OFL, Fig. 1A–c) and fiber (Fig. 1A–d). Fibers were oriented at ±45° and ±30° to the transverse plane to represent inner and outer AF (I/OAF) [2, 7].

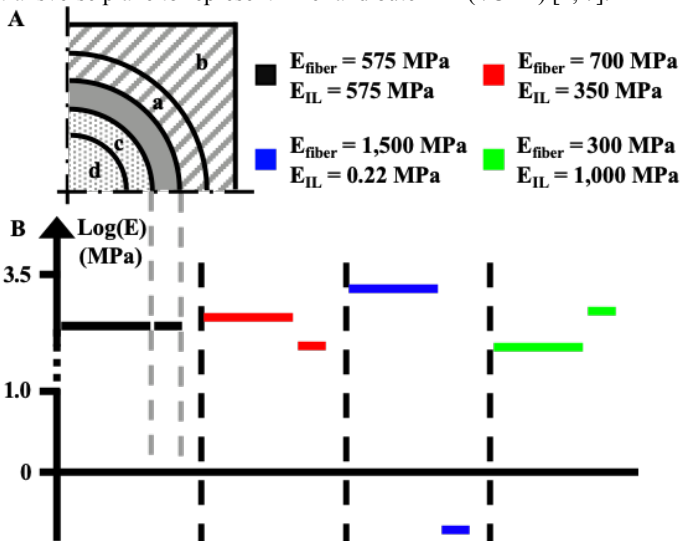

Figure 1: A. Model setup B. Investigated interfacial mechanical gradients. The same color scheme is used in all following figures.

Four interfacial mechanical gradients were investigated. *No gradient* specimens (Fig. 1B–black) had no interfacial mechanical

gradient and served as the baseline. *Gradient* specimens (Fig. 1B–red) had a linearly decreasing modulus from the fibers to the matrix. IL modulus of the *soft IL* (Fig. 1B–blue) and *stiff IL* (Fig. 1B–green) specimens was defined to be the same as matrix modulus and 1 GPa, respectively. Matrix modulus was 0.22 MPa for all models [8]. Damage mechanics was examined under a strain-based reactive damage framework [9]. The material parameters of the baseline were calibrated to single-lamellar uniaxial tensile test data using a multiscale framework and all the remaining specimens were calibrated to the same bulk stress-strain response such that the effect of interfacial mechanical gradient on sub-tissue level failure mechanics can be investigated [6, 9].

Each model was loaded in a two-step process. Triphasic free swelling in physiological saline was followed by a 25% uniaxial tension [10]. To calculate stress-strain response and damage accumulation, the point pre-tension and post-swelling was defined as the reference configuration. Stress-strain distribution was evaluated at 15% engineering strain; damage accumulation was assessed during tension.

RESULTS

Calibrated fiber and IL modulus were summarized in Fig. 1. Bulk stress-strain responses were identical in IAF and OAF, respectively (Fig. 2). Predicted damage initiated earlier in OAF than IAF for all interfacial mechanical gradients (Fig. 3). In all specimens, predicted damage initiated earlier within IL while more accumulated damage was observed around the interfacial layer (*i.e.*, OFL, IL, and IML, Fig. 3–solid versus dashed lines). Earliest and latest strain at damage initiation ($\varepsilon_{ini.}$) was predicted for the soft IL model at <5% and for the stiff IL model at >15%. In both IAF and OAF, an increased IL modulus resulted in a delayed predicted fiber and IL damage initiation but had no effect on predicted matrix damage initiation, as well as the rate of damage accumulation in the fibers, IL, and the matrix (Fig. 3).

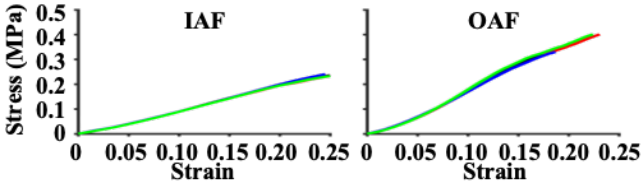

Figure 2: Calibrated bulk stress-strain response of IAF and OAF

Stresses and strains were larger in OAF than IAF. In both IAF and OAF, an increased IL modulus resulted in a more uniform fiber stress profile (Fig. 4A–Fiber panel, green line). However, all specimens shared a similar fiber strain profile (Fig. 4B–Fiber panel). While stress increased monotonically from the fiber-IL interface to mid-IL and decreased monotonically from mid-IL to the matrix in no gradient and stiff IL specimens, a monotonically decreased stress was observed from the fiber-IL interface to the matrix in gradient and soft IL specimens (Fig. 4A–IL panel). Comparable strain profiles were observed in IL except for the soft IL specimen, which had a larger strain mid-IL (Fig. 4B–IL panel). Matrix stress-strain distributions were identical across all models in each anatomical region (Fig. 4–Matrix panel).

DISCUSSION

We investigated the effect of sub-tissue level interfacial mechanical gradient on tissue failure mechanics using a multiscale, structure-based FEM based on AF. Without a fiber-matrix interfacial mechainical gradient or with an IL that was less stiff than the fibers, the fiber-IL interfacial stress was larger than the fiber stress (Fig. 4A–Fiber panel), and the fiber-IL interfacial stress was up to twice of the fiber stress in IAF in stiff IL specimen. The inclusion of a stiffer interfacial layer eliminated this stress difference, resulting in a more uniform fiber stress profile (Fig. 4A–Fiber panel, green line) despite its larger fiber-IL modulus difference (700 versus 350 MPa (gradient specimen)), as well as a delayed damage initiation ($\varepsilon_{ini.,\ stiff\ IL} > 3x\ \varepsilon_{ini.,\ soft\ IL}$). In each anatomical region, regardless of IL modulus differences, comparable strain profiles were observed (Fig. 4B) while matrix stress distribution and predicted damage initiation were identical (Fig. 3, Fig. 4A–Matrix panel). These findings suggested that tissue failure behaviors might be dominated by the fiber-IL interfacial stress, and the inclusion of a stiff IL could potentially improve tissue failure properties by creating a more uniform fiber stress profile that minimized the fiber-IL interfacial stress.

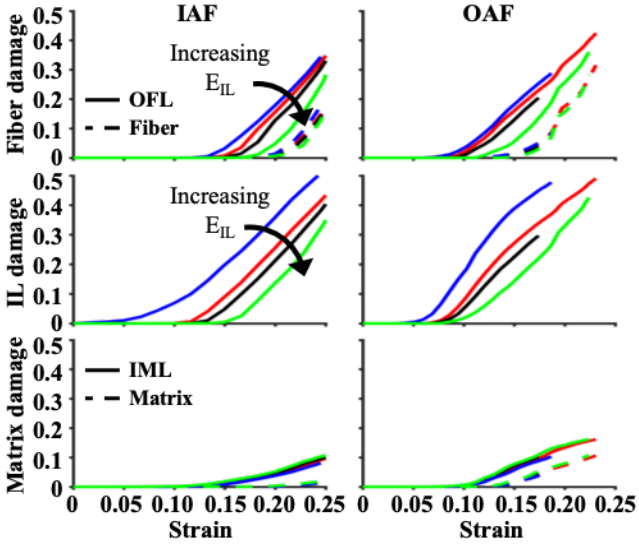

Figure 3: Damage accumulation for IAF and OAF during tension

Contrary to the previous work on tendon-bone interfaces, which suggested that stress concentration should be minimized for a more compliant interfacial system [1], a stress concentration at mid-IL was observed in the stiff IL specimen (Fig. 4A–IL panel, green line). This difference might be attributed to the length scale investigated (sub-tissue level versus tissue/joint level) and differences caused by tissue swelling and fiber orientations (AF versus tendon), which will be included in the future work.

In conclusion, this study adapted our previously developed and validated FEM to examine the sub-tissue level mechanics at the fiber-matrix interface. We found that the interfacial stress at the fiber-IL interface played a significant role in tissue failure behaviors while the inclusion of a stiff interfacial layer can potentially improve the tissue failure properties. These observations are valuable for guiding biomimetic strategies aimed at designing such hard-soft interfaces.

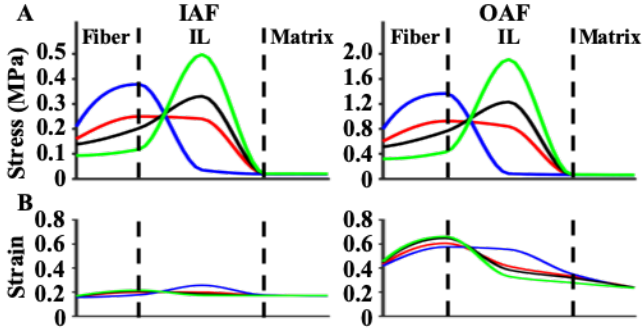

Figure 4: Stress-strain distribution for IAF and OAF

REFERENCES

[1] Liu YX+, *Mech Mater*, 44:83-92, 2012. [2] Cassidy JJ+, *Connect Tissue Res*, 23(1):75-88, 1989. [3] Kokkinis D+, *Adv Mater*, 30(19):1705808, 2018. [4] Bezci SE+, *JOR Spine*, 2(3), 2019. [5] Mueller J+, *Adv Mater*, 1705001, 2018. [6] Zhou M+, *BMMB*, 2019. [7] Marchand FR+, *Spine*, 15(5):402-410, 1990. [8] Holzapfel GA+, *BMMB*, 3(3):125-140, 2005. [9] Nims RJ+, *Interface Focus*, 6(1):20150063, 2016. [10] Lai WM+, *J Biomech Eng*, 113(3):245-258, 1991.